

EXPERIMENTAL INVESTIGATION OF THERMOACOUSTIC INSTABILITIES FOR A MODEL COMBUSTOR WITH VARYING FUEL COMPONENTS

X.Y. Zhang, H. Zhang, and M. Zhu*

Key Laboratory for Thermal Science and Power Engineering
Department of Thermal Engineering, Tsinghua University, Beijing 100084, China
Email: zhumin@tsinghua.edu.cn

ABSTRACT

In this study, a combustion facility was constructed that includes a flexible fuel supply system to produce synthesis gas using a maximum of three components. The rig with lean premixed burner is able to operate at up to 5 bars. The length of the inlet plenum and the outlet boundary conditions of the combustion chamber are adjustable. Experiments were carried out under a broad range of conditions, with variations in fuel components including hydrogen, methane and carbon monoxide, equivalence ratios, thermal power and boundary conditions. The dynamic processes of self-excited combustion instabilities with variable fuel components were measured. The mechanisms of coupling between the system acoustic waves and unsteady heat release were investigated. The results show that instability modes and flame characteristics were significantly different with variations in fuel components. In addition, the results are expected to provide useful information for the design and operation of stable syngas combustion systems.

INTRODUCTION

Reduction of pollution and greenhouse gases requires the development of alternative fuel power systems such as integrated gasification combined cycle (IGCC) and biomass integrated gasifier-combined cycles (BIG-CC). These systems utilize coal and biomass resources with higher efficiency and lower emissions. The combustion of syngas derived from coal, biomass and waste is significantly different from the combustion of typi-

cal gas turbine fuels such as natural gas and fuel oils [1]. For natural gas, the latest lean premixed Dry Low NO_x (DLN) technique can achieve less than 5 ppmvd NO_x emissions. The high hydrogen content in syngas has complicated the resolution. Although the addition of hydrogen gives a wider flammability range, flashback into the premixer can lead to catastrophic failure because the components in the premixer are more susceptible to overheating and damage.

In conventional syngas combustion systems, the non-premixed approaches are used to control NO_x emissions by diluting the syngas with nitrogen, steam or carbon dioxide. However, increased fuel flow and the addition of diluent substantially increase the overall mass flow through the turbine. This can create back-pressure to the compressor and can bring the engine close to surge conditions. In addition, the non-premixed combustors have a reacting limitation when surplus inert diluent is added for further emission reduction. In practice, the best emission level achieved for syngas combustors is between 10 and 20 ppmvd NO_x. Therefore, it is desirable to explore the feasibility of using hydrogen enriched fuels within industrial DLN gas turbine burners.

DLN technology is limited under some conditions because lean premixed combustion leads to strong coupling between pressure and heat release oscillations. The oscillations are driven by the resonant interaction between acoustic waves and unsteady heat releases. Pressure waves can become so intense that they cause unbearable noise, vibration and even structural damage. It is well known that combustion oscillation is a system-coupled phenomenon, which involves the interaction of pressure waves,

*Address all correspondence to this author.

unsteady combustion, fuel/air supplies, and geometry of combustors.

A great deal of experimental research has been conducted on thermoacoustic oscillation in a model combustor using conventional fuels over the last decade [2]. Langhorne et al. [3, 4] investigated combustion instability on a laboratory rig, in which a premixed flame burns in a duct, and developed a theoretical model to determine the frequency and mode shape of the instability. Schildmacher et al. [5] studied thermoacoustic instabilities and their interaction with the periodic fluctuations of the velocity and pressure in a single model gas turbine burner. Durox et al. [6] measured the nonlinear flame response to acoustic velocity oscillations under different configurations. Hield et al. [7] presented an experimental and theoretical investigation of the response of a turbulent premixed flame during the thermoacoustic limit cycle. Kim et al. [8] experimentally compared the nonlinear response of swirl stabilized flames to equivalence ratio oscillations. In recent years, many efforts have been made to develop a combustor with synthesis gases [9]. Lieuwen et al. studied flashback and lean blowout characteristics of $H_2/CO/CH_4$ mixtures. The results show that the percentage of H_2 in the fuel dominates the blowout characteristics and can be captured with classical Damköler number [10, 11]. Lee et al. [12] investigated the combustion performance of syngas, and the results were compared with those of methane combustion. Daniele et al. [13] analyzed turbulent flame speed data for high hydrogen-containing fuel gas mixtures; the results indicated a high risk for flame flashback. Boschek et al. [14] experimentally investigated the effects of fuel variability on turbulent premixed flames at gas turbine relevant conditions. Richards et al. [15] measured stability maps and heat release distributions of natural gas and natural gas/propane mixtures. In addition, the methods to reduce emission or control instability with a hydrogen injection modulator were investigated [16, 17].

While the thermoacoustic instabilities of lean premixed combustion have been intensively investigated, little experimental data is available for thermoacoustic instabilities in a fixed geometry for various fuels. The objective of this work is to investigate the effects of blended fuel components, mainly methane, hydrogen, carbon monoxide and nitrogen, upon combustion oscillations in a fixed geometry system. The results may give the insight into the interaction mechanisms between fuel components, combustion dynamics and acoustic waves and provide definitive experimental data for theoretical study and model validation. In the next section, the experimental setup and diagnostics are described. Then, the experimental results for natural gas are presented. The results for $CH_4/H_2/N_2$, H_2/CO and H_2/N_2 synthesis gases are described in Sections 4-6 respectively. Finally, general conclusions and further work are discussed.

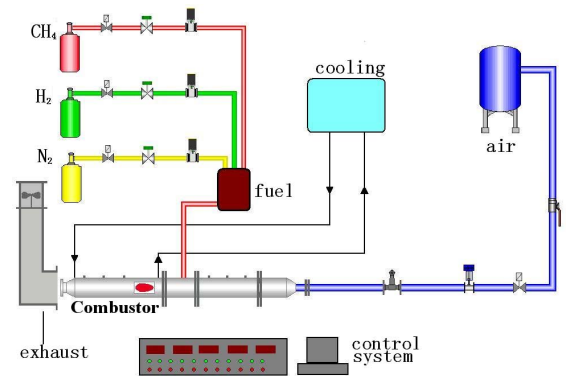


FIGURE 1. Schematic of the experimental apparatus.

FACILITIES

The experimental rig is shown in Fig. 1. It is a generic combustor designed to model the fuel injection/premix ducts of an industrial gas turbine. The geometries of the plenum and combustor have been simplified to be cylindrical pipes. A steady air flow is supplied to the plenum through a choked plate. This effectively decouples the air supply from pressure fluctuations in the working section, enabling air to be supplied at a constant mass flow rate while providing a well-defined acoustic boundary condition. The area of exit nozzle is adjustable so that the choking boundary condition can be implemented. The inner diameter and length of the combustor are 120 mm and 850 mm, respectively. There are quartz windows in the combustion zone for optical access.

Air and fuel are fully mixed through the flow path before entering the combustor. The fuel supply system supplies a gaseous mixture with a maximum of three components in an arbitrary percentage. All gas flow rates are monitored with mass flow controllers (Bronkhorst). Figure 2 shows a cross-section of the swirling injector. The configuration employs a swirler and mixing tubes in a sudden expansion dump combustor. The swirler has eight curved vanes with an 52° fixed angle and a swirler number of 0.88. The premixer consists of five tubes that are located 20 mm behind the exit of the injector. The tubes have a diameter

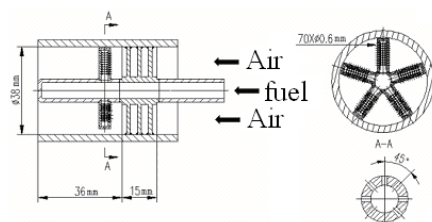


FIGURE 2. Sketch of the swirling injector.

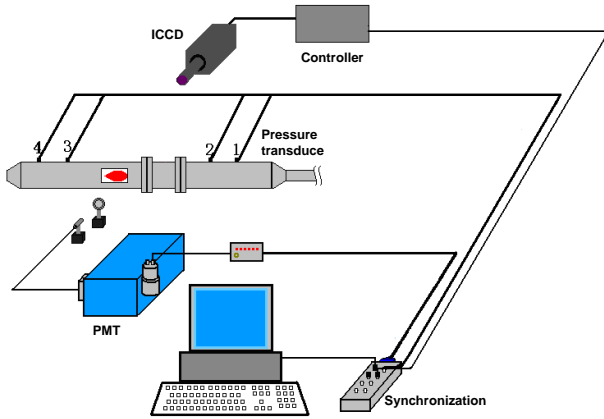


FIGURE 3. Measurement system used for the combustion instability studies.

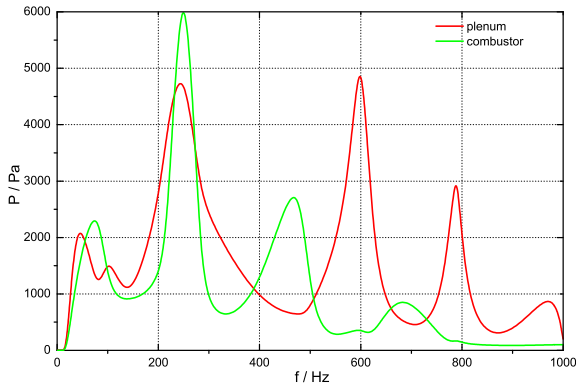
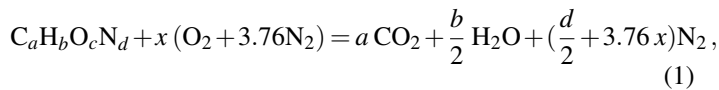


FIGURE 4. Resonance frequencies in the plenum and the combustor.

of 0.5 mm, with 70 holes in each tube. Fuel is ejected perpendicular to the center axis of the swirler. For a blended fuel given by $C_aH_bO_cN_d$, the stoichiometric relationship can be expressed as:



where $x = a + b/4 - c/2$. We assume that for each mole of O_2 in air, there are 3.76 mole of N_2 . For the given air and fuel mass flow rate, m_a and m_f , the equivalence ratio can be written as:

$$\phi = 4.76\left(a + \frac{b}{4} - \frac{c}{2}\right) \frac{MW_a m_f}{MW_f m_a}, \quad (2)$$

where MW_f and MW_a are the molecular weights of the fuel and air, respectively.

As shown in Fig. 3, different instruments and techniques were applied to identify the dynamic relationship between unsteady pressure waves and heat release rates. The semi-infinite tube method was used for the dynamic pressure measurements. Four PCB pressure transducers (PCB112A22) measured inlet plenum and combustor pressure at a variety of locations. To examine the instantaneous radiation emitted from chemiluminescence OH^* radicals, a spectrometer was used to evaluate the heat release rate of the flame. The UV narrow band filter was centered at 308 nm. The optical signal from the spectrometer was sampled synchronously with the dynamic pressure signals through the data acquisition module, NI-6123, operating LabVIEW software. The spatial distribution of OH^* emission was obtained with an intensified CCD camera (PI-MAXII-5MHz) and a 308 nm interferential filter. A high-speed camera (Phantom V210 with SAM-3-USB) was also used to obtain visible light images of flame. With the same reference as dynamic pressure/optical signals, a phase-locked technique was used to obtain the information over a number of phase angles in one cycle.

The resonant frequencies of the combustion system are measured with a loudspeaker fixed in the inlet of the plenum. The results of amplitudes of dynamic pressure within combustor and plenum are shown in Fig. 4. In the plenum, the fundamental mode is approximately 50 Hz. The fundamental and the higher harmonic resonant modes of the combustor are around 90 Hz, 270 Hz, 450 Hz, and 720 Hz, respectively.

NATURAL GAS

At the beginning, combustion characteristics of natural gas in the model combustor were examined with the outlet open. The experiment was conducted by varying the equivalence ratio. The stability map is shown in Fig. 5. From the figure, two distinct behaviors are observed. When the equivalence ratio is leaner than 0.65, the frequency of pressure oscillation is approximately 510 Hz, and the Sound Pressure Level (SPL) is 140-150 dB. A sudden increase occurs when the equivalence ratio is richer. The frequency of the pressure oscillation is 90 Hz,

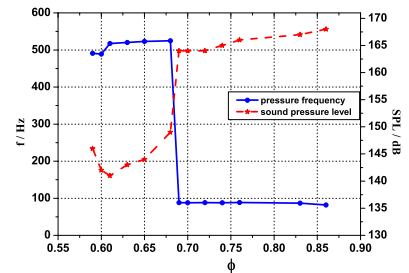


FIGURE 5. Variations of frequency and SPL with the equivalence ratio at the air flow rate 40 g/s under open outlet condition.

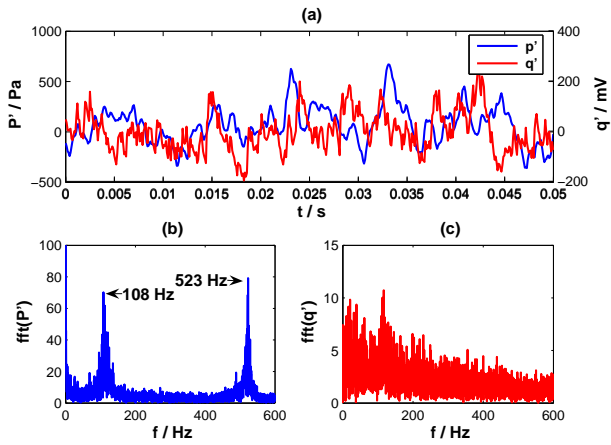


FIGURE 6. Time traces and spectra of dynamic pressure and OH* chemiluminescence at the air mass flow 40 g/s and the equivalence ratio 0.65 with open outlet.

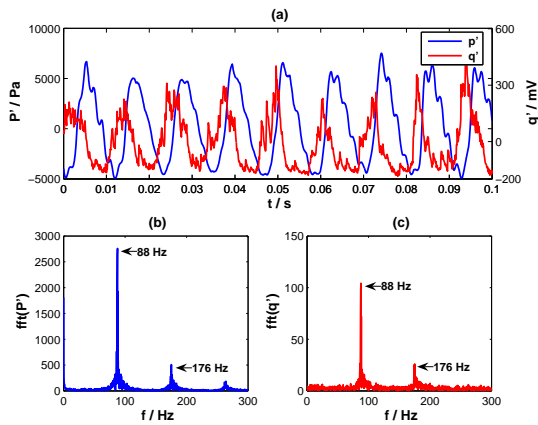


FIGURE 7. Time traces and spectra of dynamic pressure and OH* chemiluminescence at the air mass flow 40 g/s and the equivalence ratio 0.74 with open outlet.

and the SPL is 165-170 dB. Similar phenomena were reported in reference [18]. To understand the mechanisms, the time traces of simultaneously measured dynamic pressure and OH* chemiluminescence signals are demonstrated in Fig. 6(a). The corresponding Fourier transformations are also shown in Figs. 6(b)-(c). In stable modes, the dynamic pressures are at the frequencies of 100 Hz and 500 Hz. For an unsteady heat release rate, no clear dominating frequencies are observed. These results indicate that there is no correlation between fluctuating pressure and unsteady heat release. When the equivalence rate is 0.74, compared with pressure and heat release rate time traces in Fig. 7(a), it can be seen that both oscillations occurred at around 90 Hz. Their phase angle difference is less than 90°. According to Rayleigh's criteria, the thermoacoustic oscillation is built, and the strong un-

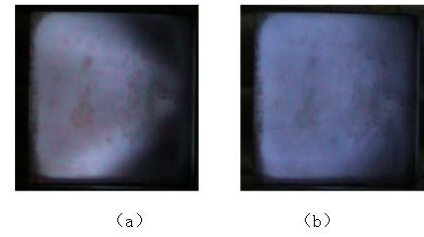


FIGURE 8. Flame images with digital camera at (a) stable mode (b) unstable mode.

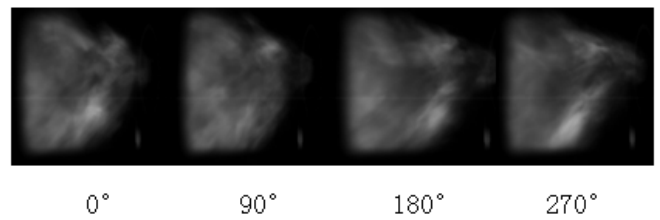


FIGURE 9. High speed camera images from a cycle of the acoustic waves at the air mass flow 40 g/s and the equivalence ratio 0.65 with open outlet.

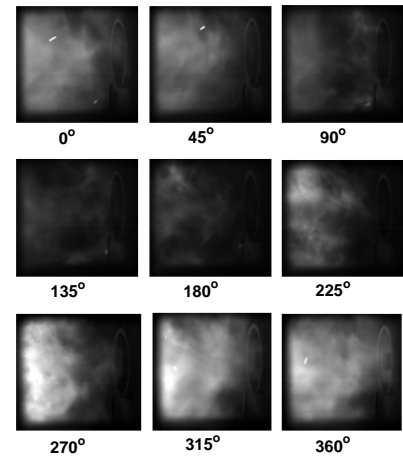


FIGURE 10. High speed camera images from a cycle of the thermoacoustic oscillation at the air mass flow 40 g/s and the equivalence ratio 0.74 with open outlet.

steady interactions between the flame and pressure cause large amplitudes of pressure oscillations.

The stable and unstable flames were observed using a digital camera. As shown in Fig. 8, the flame has a conical shape in stable mode. In comparison, in the unstable mode, the flame fills the quartz window, and the fringe of the flame cannot be identified. The dynamic details were examined with a high-speed

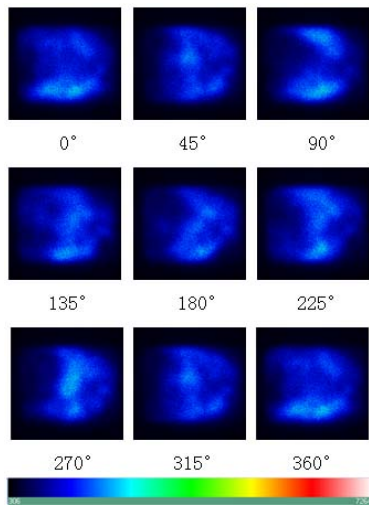


FIGURE 11. ICCD images from a cycle of the acoustic waves at the air mass flow 40 g/s and the equivalence ratio 0.62 with open outlet.

camera capable of 5000 frame/s. Figure 9 gives the variations of the flame distribution over one pressure oscillation cycle in a stable mode. The flame is anchored at the edge of injector despite the presence of weak pressure oscillation. The chemical reactions take place within the recirculation zone behind the backward facing step of the dump combustor. For the unstable mode in Fig. 10, the flame bottom leaves the swirler exit and reattaches periodically at a frequency of 90 Hz. With ICCD, the phase-resolved information on the dynamic behavior of chemiluminescence OH* in a cycle for both stable and unstable modes is demonstrated in Figs. 11 and 12, respectively. For the stable mode in Fig. 11, the equivalence ratio is 0.62 and the pressure oscillation frequency is 510 Hz. The distribution of OH* is in a V shape and does not cause any change. For the unstable mode in Fig. 12, the equivalence ratio is 0.68 and the pressure oscillation frequency is 87 Hz. Distinct variations are observed. The intensity of OH* is the weakest in phase 180° and reaches the maximum around 270° – 315°. In this situation, the strong coupling between heat release and pressure is established.

The influence of the outlet boundary conditions on combustion instability was investigated by varying the size of the exit nozzle. Three exit nozzle diameters, 25 mm, 22 mm and 12.5 mm, were selected. The exit is choked when the nozzle diameter is 12.5 mm. For a constant air flow rate 30 g/s, the same experiments were conducted for a broad range of equivalence ratios from 0.55 to 0.87. The results of instability are shown in Fig. 13; thermoacoustic oscillations exist whole range of the equivalence ratios in choking conditions. For a larger exit nozzle size, the oscillation vanishes with decreasing equivalence ratio. The frequencies of oscillation are around 80 Hz and have no in-

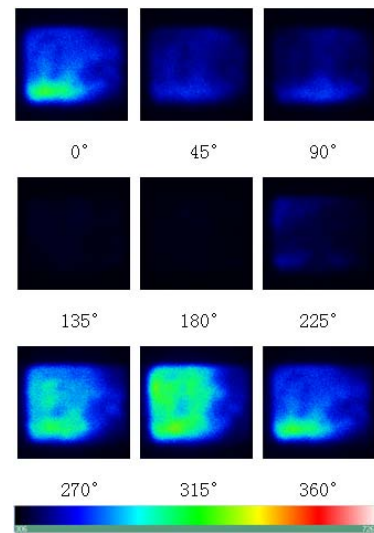


FIGURE 12. ICCD images from a cycle of the thermoacoustic oscillation at the air mass flow 40 g/s and the equivalence ratio 0.68 with open outlet.

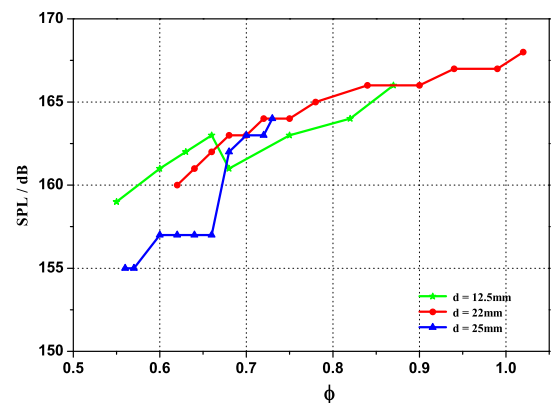


FIGURE 13. Variations of SPL with the size of exit nozzle at the air flow rate 30 g/s.

stability mode shift. From Fig. 13, the oscillation SPL will rise when the equivalence ratio increases.

NATURAL GAS/ HYDROGEN/ NITROGEN

The combustion instabilities of natural gas blended with hydrogen and nitrogen were studied. Hydrogen has a lower heating value (LHV) of approximately 10.77 MJ/m³. Moreover, hydrogen is easy to ignite and has a large flame propagation speed and a small quenching distance. Blending traditional hydrocarbon fuels with hydrogen significantly improves flame stability during lean combustion and reduces NO_x emissions. These properties affect flame stability, combustor acoustics and other important

Case	CH ₄ : H ₂ : N ₂	ϕ	LHV (MJ/m ³)	Wobbe index (MJ/m ³)
1	4 : 0 : 1	0.58	28.64	38.47
2	3 : 1 : 1	0.58	23.63	37.05
3	2.5 : 1 : 1	0.50	22.28	35.83
4	2 : 2 : 1	0.58	18.63	35.64
5	1 : 2.5 : 1	0.50	13.94	33.46
6	1 : 3 : 1	0.41	13.62	34.22

TABLE 1. Fuel compositions of the mixtures used in the experiments.

parameters [19]. Table 1 summarizes the fuel compositions of the mixture with a fixed 20% nitrogen volume percentage. In Tab. 1, the Wobbe index is an indicator of the interchangeability of fuel gases for a given pressure drop, and is defined as

$$\text{Wobbe Index} = \frac{\sum X_i \cdot \text{LHV}_i}{\sqrt{\sum X_i \cdot \rho_i / \rho_{\text{air}}}}, \quad (3)$$

where X_i is the mole fraction of each fuel component in a blended fuel, and LHV is the fuel lower heating value. The specific gravity of fuel is normalized by the density of air at standard conditions.

From cases 1 to 6, with increasing hydrogen content, the blended fuel turns from a high-Btu gas to medium-Btu gas. For selected cases, the variations of flame shapes in stable mode are shown in Fig. 14. Compared with pure natural gas in Fig. 8(a), the length of the flame is shorter and closer to the nozzle exit with increasing hydrogen content and flame speed. When the flame speeds are larger with increasing hydrogen content, flashback occurs. From Fig. 14(d), the injector is burnt red. The flashback can lead to combustor hardware damage and must be avoided in practice.

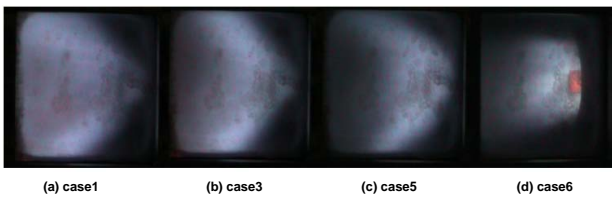


FIGURE 14. Stable flame images with the variations of the fuel compositions listed in Tab. 1.

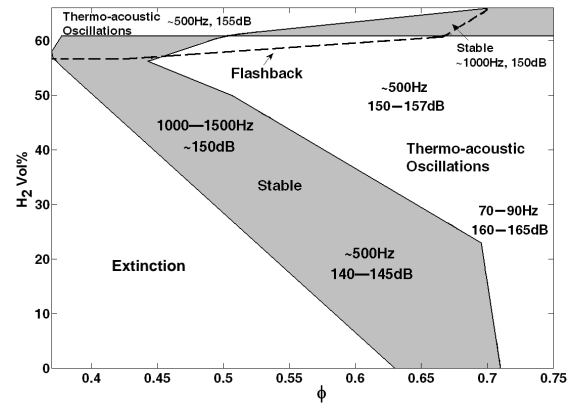


FIGURE 15. Stability map with the equivalence ratio and the hydrogen content of the CH₄/H₂/N₂ blended fuels.

In the experiments, the effects of equivalence ratio on the combustion were studied by adjusting the air flow rate and fixing the fuel contents. For a given constant blended fuel mass flow rate, the stability map as the functions of the equivalence ratio and the hydrogen content can be obtained. Figure 15 demonstrates the stability map for hydrogen percentage from 0 to 66 Vol% and the corresponding thermal power is from 83.8 kW to 40 kW. The grey color indicates the stable zone is the only location where acoustic waves are detected. The above dash line refers to the flashback area. The higher the hydrogen content, the wider the flashback region. From Fig. 15, the extinction limit gradually reduces with increasing hydrogen content in the fuel mixture. At the same time, the range of thermoacoustic instability increases. A similar result was also seen from experiments in reference [18]. When the hydrogen content is less than 55 Vol%, the frequencies in unstable modes are in the range of 70-90 Hz. This characteristic is consistent with the results of pure natural gas discussed in the previous section. In stable modes, the frequencies of acoustic waves are approximately 500 Hz. When the hydrogen content is more than 55 Vol%, the unstable modes jump to 500 Hz, and the stable modes increase to frequencies between 1000-1500 Hz. The effects of the equivalence ratio on combustion oscillation in the flashback zone show an opposite tendency. In this zone, combustion oscillation takes place in the relatively small equivalence ratio and transfers to a stable state when the equivalence ratio increases.

Two typical time traces of dynamic pressure and OH* chemiluminescence signals are illustrated in Figs. 16 and 17. Figure. 16 shows the results of case 4, in which the stability boundary is approximately 0.6. When the equivalence ratio is 0.58, the dominating frequency of pressure fluctuations is 1016.9 Hz with harmonics near 500 Hz and 1500 Hz. For the heat release rates shown in Fig. 16(c), there is no dominating frequency in its spectrum. Therefore, the heat release rate can be described as low-band noise. In case 6, the combustor sys-

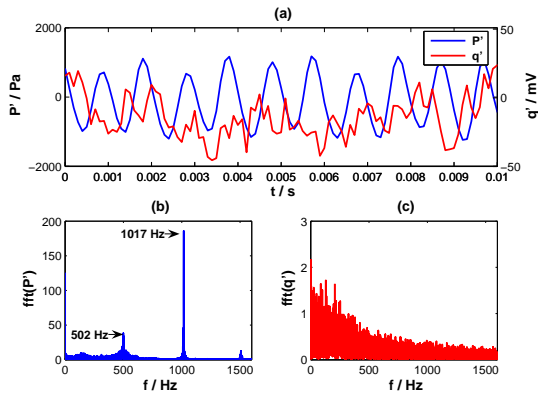


FIGURE 16. Time traces and spectra of dynamic pressure and OH* chemiluminescence at the air mass flow 35 g/s and the equivalence ratio 0.80 with the H₂ 40 Vol% of CH₄/H₂/N₂ blended fuels.

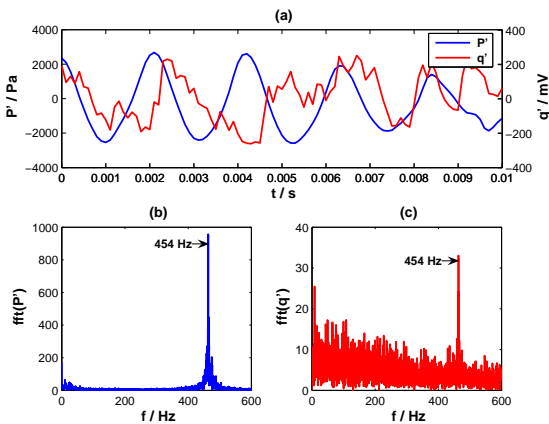


FIGURE 17. Time traces and spectra of dynamic pressure and OH* chemiluminescence at the air mass flow 50 g/s and the equivalence ratio 0.41 with the H₂ 60 Vol% of CH₄/H₂/N₂ blended fuels.

tem transfers to the unstable modes when the equivalence ratio is 0.41. Figure 17 shows that both pressure and heat release fluctuations are in the same frequencies, and the SPL is more than 5 dB higher than under stable conditions. When the equivalence ratio increases to 0.6, the strong oscillation fades away, and the acoustic frequency switches to 1007.8 Hz. At the same time, flashback will vanish with increasing equivalence ratio and flame speeds. This proves that thermoacoustic oscillation enhances flashback due to the close coupling between flame speed, unsteady heat release and acoustic waves. The phase-resolved images of chemiluminescence OH* for the unstable modes of case 6 are shown in Fig. 18. In comparison with Fig. 12, the area of radical OH* is much closer to the injector.

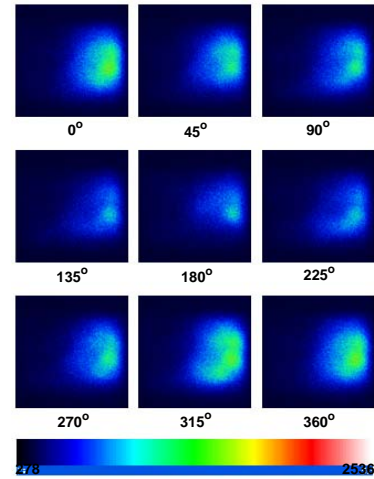


FIGURE 18. ICCD images from a cycle of the thermoacoustic oscillation with the H₂ 60 Vol% of the CH₄/H₂/N₂ blended fuel.

CARBON MONOOXIDE/ HYDROGEN

Syngas is primarily composed of hydrogen and carbon monoxide, but has a third of the heating value of methane (natural gas). Typical syngas fuels used for this study with their compositions are listed in Table 2. The selected flame images shown in Fig. 19 were taken using a high speed camera for different hydrogen and carbon monoxide volume ratios. Compared with Fig. 14, the flames are more like jet flames, and the strong recirculation zone around the dump plane is not observed. Similar phenomena are reported in reference [12]. The Lewis number of syngas with high hydrogen is less than unity, and the variations of hydrogen content change the diffusivity of the mixture and flame characteristics [20]. The laminar flame speed of the CO/air mixture is very sensitive to small additions of hydrogen, which implies that the main CO oxidation reaction ($\text{CO} + \text{OH} = \text{CO}_2 + \text{H}$) is important. On the other hand, flame

Case	H ₂ : CO	ϕ	LHV (MJ/m ³)	Wobbe index (MJ/m ³)
1	1 : 0.67	0.23	11.51	29.73
2	1 : 1	0.25	11.70	26.92
3	1 : 3	0.24	12.17	19.87
4	1 : 6	0.22	12.36	16.85

TABLE 2. Syngas compositions used in the experiments.

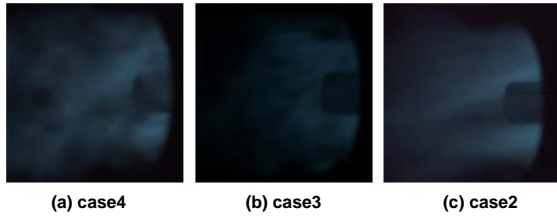


FIGURE 19. Stable flame images with the variations of the fuel compositions listed in Tab. 2.

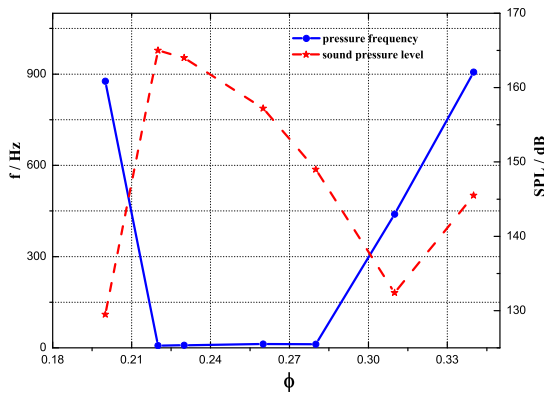


FIGURE 20. Variations of frequency and SPL with the equivalence ratio for the blended fuel $H_2 : CO = 1 : 6$.

speeds for mixtures with high hydrogen contents are less sensitive to small CO additions. Further investigation should be conducted to understand the interaction mechanisms between fuel components and flame dynamics.

Experiments were performed with a fixed total fuel mass flow rate and each gas component. The influence of the equivalence ratio on combustion instability was studied with an adjustable air mass flow rate. The stability map of case 4 in Tab. 2 is illustrated in Fig. 20. In this case, carbon monoxide is predominant. Although the low flammability limits in air are large (12.5 in volume), a small amount of hydrogen content significantly improves flammability. From the Fig. 20, the combustion is unstable, and the equivalence ratio ranges between 0.21 and 0.30. In this range, the 8.5 Hz low frequency unstable mode is detected, and its SPL reaches as high as 166 dB. The time traces of pressure and OH^* chemiluminescence signals are shown in Fig. 21. The figure shows that the heat release is very unstable and is in the same phase as the pressure signal. The unstable fre-

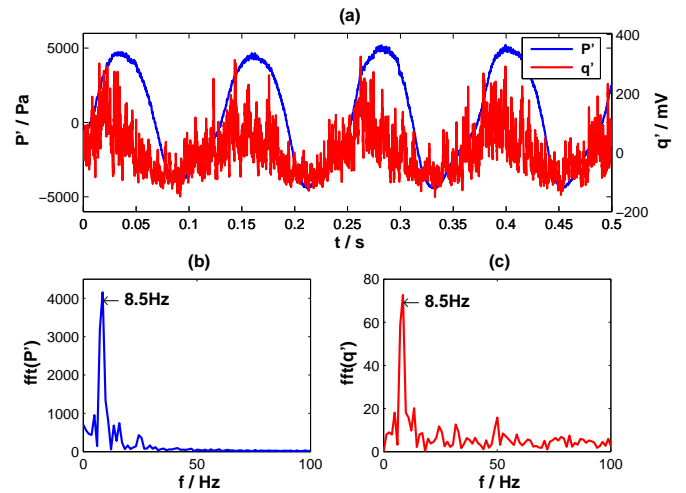


FIGURE 21. Time traces and spectra of dynamic pressure and OH^* chemiluminescence at the air mass flow 38 g/s and the equivalence ratio 0.22 for the blended fuel $H_2 : CO = 1 : 6$.

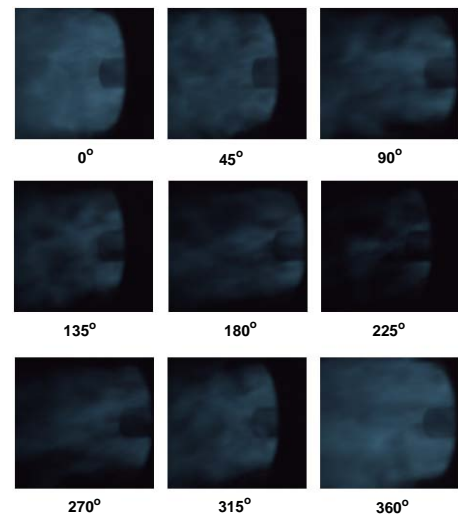


FIGURE 22. High speed camera images from a cycle of the thermoacoustic oscillation for the blended fuel $H_2 : CO = 1 : 6$.

quency is much lower than the order of the Helmholtz resonator mode, which is about 137 Hz. This phenomena may be a result of the low frequency relationship with vortices induced by jet flames. Moreover, due to low caloric value, the intensive fluctuations of the flame surface are observed, which tend to generate strong heat release fluctuations. With coupled unsteady pressure and heat release, the intensive thermoacoustic oscillation is established.

The phase-resolved flame images from the high-speed camera for the unstable modes of case 4 are shown in Fig. 22. In com-

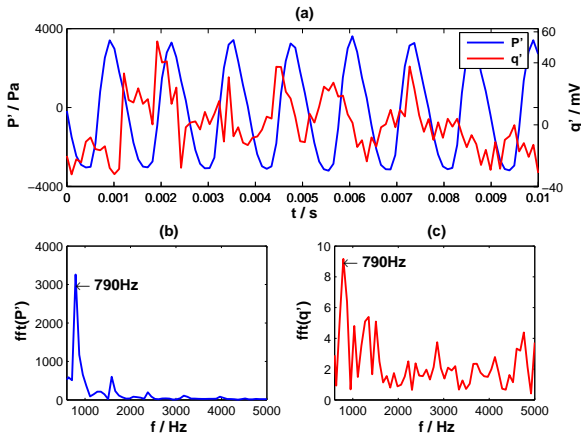


FIGURE 23. Time traces and spectra of dynamic pressure and OH* chemiluminescence at the air mass flow 30 g/s and the equivalence ratio 0.23 for the blended fuel $H_2 : CO = 3 : 2$.

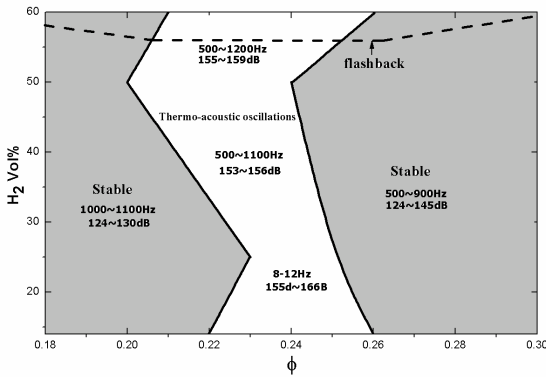


FIGURE 24. Stability map with the equivalence ratio and the hydrogen content of the CO/H₂ blended fuels.

parison with the natural gas unstable case in Fig. 10, the flame dynamics and thermoacoustic oscillation frequencies are different from those in the natural gas cases. In this circumstance, the unsteady flame periodically spreads to the injector nozzle, instead of periodically leaving and re-attaching to the injector nozzle in the natural gas unstable modes.

With increasing hydrogen contents in the gas mixture, the unstable modes are shifted to the higher frequencies. Figure 23 shows the time traces of pressure and OH* chemiluminescence signals when the volume ratio between CO and H₂ is 0.67. The oscillation frequency is 790 Hz. In the experiment, the oscillation frequencies reach as high as 1200 Hz when the hydrogen volume percentage exceeds 50%. The stability map for the functions of equivalence ratio and hydrogen content is shown in Fig. 24. From the figure, the unstable zone is confined in a narrow range around a mean equivalence ratio of 0.24. With increasing hydrogen content, the unstable range is slightly enlarged. In com-

parison with the result for the natural gas/hydrogen mixture in Fig. 15, both unstable frequencies are as high as 500 Hz (or its harmonic) when the hydrogen is richer. In addition, flashback will happen when the hydrogen volume percentage is near 60%. A higher flame speed has a tendency to excite high frequency thermoacoustic oscillations. If the hydrogen content is decreased, the unstable modes are 70 Hz and 8 Hz, respectively. These results might be caused by the different flame dynamics and their interaction mechanisms with acoustic waves.

HYDROGEN/ NITROGEN

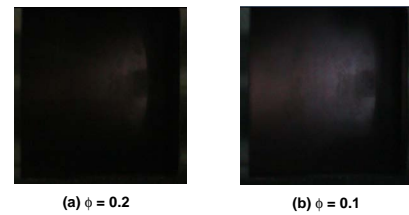


FIGURE 25. Stable hydrogen flame images with the equivalence ratios of (a) 0.2 (b) 0.1.

Hydrogen, a carbon-free energy carrier, is likely to play an important role in eliminating greenhouse gas emissions. In the gas turbine industry, the prospect of premixing hydrogen and air combustion to achieve zero emissions needs to be explored. Figure 25 shows two images of hydrogen flames with the same fuel mass flow rate 0.17 g/s and air mass flow rates of 30 g/s and 60 g/s. The corresponding equivalence ratios are 0.2 and 0.1, respectively. When the hydrogen flame is very pale blue, it is almost invisible in daylight. When images displaying a large flow velocity and low flame speed are compared, a greater portion of the flame appears to be in the injector nozzle as shown in Fig. 25(b).

The effects of the equivalence ratio on thermoacoustic instability were investigated. First, the air mass flow was set as 30 g/s, and the hydrogen mass flow was modulated in the range of 0.15-0.37 g/s. The corresponding equivalence ratios are 0.17-0.43. Since hydrogen has a wide flammability range, the flame is available in the whole equivalence ratio range. The results of measuring the SPL, pressure and chemiluminescence OH* frequencies are presented in Fig. 26. The SPL is higher than 160 dB within the whole range. When the equivalence ratio is less than 0.3, both dominating frequencies of pressure and chemiluminescence OH* are 1078 Hz, and the SPL is 165 dB. When the equivalence ratio is larger than 0.3, the dominating frequencies are not identical, and the SPL slightly decreases. The time traces and spectrums

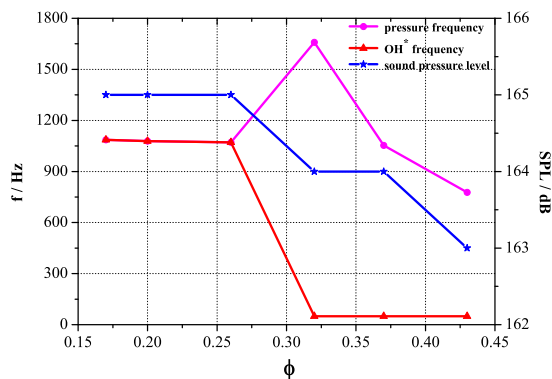


FIGURE 26. Variations of frequency and SPL with the equivalence ratio of the hydrogen flames.

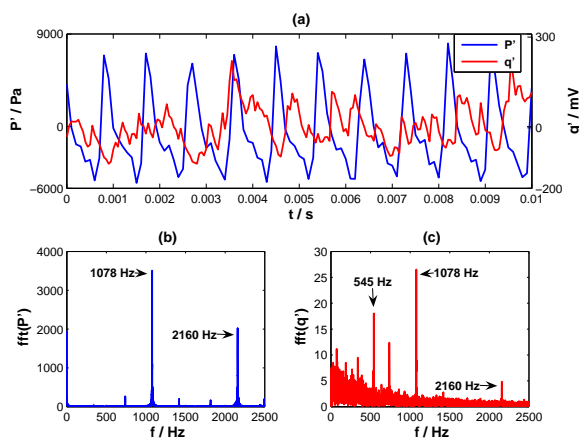


FIGURE 27. Time traces and spectra of dynamic pressure and OH* chemiluminescence at the air mass flow 30 g/s and the equivalence ratio 0.2 of the hydrogen flame.

for two typical cases were examined. From the Fig. 27, the dominating frequencies of pressure and chemiluminescence OH* are 1078 Hz. Fig. 28 shows that when the equivalence ratio is 0.37, the dominating frequencies for pressure and chemiluminescence OH* are 1053 Hz and 50 Hz, respectively. However, both cases have the same harmonic frequencies of 722 Hz. In this circumstance, the SPL is still relatively high. The thermoacoustic oscillation is not built up by the interaction between unsteady pressure and heat release in their dominating frequencies.

The effects of diluted nitrogen in hydrogen on combustion instability were also studied. For given air and hydrogen mass flow rates, the inert diluent does not change the equivalence ratio, but reduces the calorific value per volume. In the experiment, the air and hydrogen mass flow rates were 30 g/s and 60 g/s, respectively. Nitrogen flow rate was varied in the range of 0-2.43 g/s, and the corresponding calorific values were between 10.77 and 5.39 MJ/m³. The frequencies and amplitudes of oscillation with

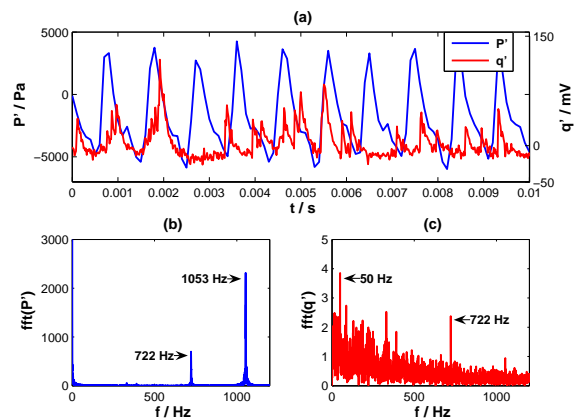


FIGURE 28. Time traces and spectra of dynamic pressure and OH* chemiluminescence at the air mass flow 30 g/s and the equivalence ratio 0.37 of the hydrogen flames.

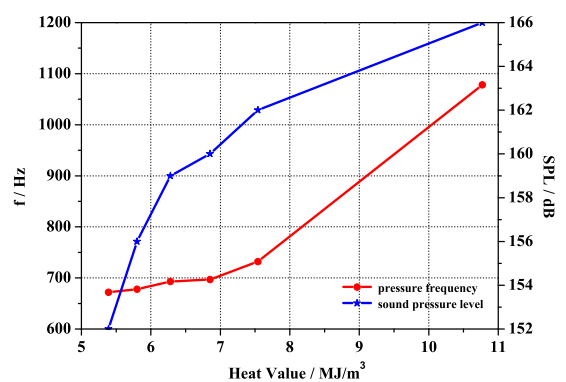


FIGURE 29. Variations of frequency and SPL with the calorific values of the H₂/N₂ blended fuels.

calorific value variation are shown in Fig. 29. The figure indicates that frequency and SPL gradually decrease with increasing nitrogen contents, but no unstable mode shift is observed.

CONCLUSIONS

In this paper, the characteristics of thermoacoustic oscillations in a premixed swirling gas turbine model combustor were studied by systematic experimental investigation. Emphasis was put on the influence of fuel composition on combustion instabilities.

Four component combinations: natural gas, natural gas/hydrogen/nitrogen, carbon monoxide/hydrogen and hydrogen/nitrogen, were selected. For natural gas, the unstable oscillation occurs with increasing equivalence ratio, and the unstable modes are approximately 88 Hz. The flame has a conical shape, and chemical reactions take place within the recirculation zone.

For the natural gas/hydrogen/nitrogen blended fuels, the stability characteristics are consistent with the pure natural gas results when the hydrogen content is less than 55 Vol%. When the hydrogen content is more than 55 Vol%, the unstable oscillation frequency jumps to 500 Hz. This change could be caused by the faster heat release fluctuations as the flame speed increases. The results indicate that the effects of the equivalence ratio on thermoacoustic oscillation in the flashback zone have an opposite direction. For the carbon monoxide/hydrogen blended fuels, the unstable modes are approximately 8.5 Hz when carbon monoxide is predominant. In this condition, the flame resembles a jet flame, and the recirculation zone around the dump plane can not be observed. The low frequency should be correlated with vortex shedding induced by reacting jet flow. With increasing hydrogen percentage in the mixture, the unstable modes shift to higher frequencies. For diluting nitrogen in hydrogen gas, frequency and SPL gradually decrease with increasing nitrogen content.

In general, the thermoacoustic instability modes obtained are in a wide range of 8-1200 Hz. For the conventional fuels, the flame stability mechanisms for swirl burners are relatively well understood. For blended fuels with hydrogen content, the characteristics of combustion dynamics vary dramatically. The variations of fuel composition change the important properties such as calorific value, flame speed, and Wobbe index, which fundamentally influence the dynamic process of combustion as well as the coupling with acoustic waves. In the future, mechanisms that lead to the thermoacoustic oscillations with varying fuel components will continue to be investigated and tools to predict the instability modes of oscillation will be developed. The results are anticipated to be useful to understand the combustion oscillation with synthesis gases in the development of control strategies.

ACKNOWLEDGMENT

This work is funded by the National Basic Research Programme of China through Grant NO.2007CB210106 whose support is gratefully acknowledged.

REFERENCES

- [1] Richards, G., McMillian, M., Gemmen, R., Rogers, W., and Cully, S., 2001. "Issues for low-emission, fuel-flexible power systems". *Prog. Energy Combust. Sci.*, **27**(2), pp. 141–169.
- [2] Lieuwen, T., and Yang, V., eds., 2005. *Combustion Instabilities in Gas Turbine*, Vol. 210. AIAA, Washington, DC.
- [3] Langhorne, P., 1988. "Reheat buzzan acoustically coupled combustion instability. Part 1. Experiment". *J. Fluid Mech.*, **193**, pp. 417–443.
- [4] Bloxsidge, G., Dowling, A., and Langhorne, P., 1988. "Reheat buzzan acoustically coupled combustion instability. Part 2. Theory". *J. Fluid Mech.*, **193**, pp. 445–473.
- [5] Schildmacher, K., Koch, R., and Bauer, H., 2006. "Experimental Characterization of Premixed Flame Instabilities of a Model Gas Turbine Burner". *Flow, Turbulence and Combustion*, **76**, p. 177C197.
- [6] Durox, D., Schuller, T., Noiray, N., and Candel, S., 2009. "Experimental analysis of nonlinear flame transfer functions for different flame geometries". Vol. 32, pp. 1391–1398.
- [7] Hield, P., Brear, M., and Jin, S., 2009. "Thermoacoustic limit cycles in a premixed laboratory combustor with open and choked exits". *Combust. and Flame*, **156**, pp. 1683–1697.
- [8] Kim, K., Lee, J., and Quay, B.D. and Santavicca, D., 2010. "Experimental Investigation of the Nonlinear Response of Swirl Stabilized Flames to Equivalence ratio Oscillations". No. GT2010-23023, Proceedings of ASME Turbo Expo 2010.
- [9] Lieuwen, T., Yang, V., and Yetter, R., eds., 2010. *Synthesis Gas Combustion Fundamentals and Applications*. CRC Press, London.
- [10] Zhang, Q., Noble, D., Meyers, A., Xu, K., and Lieuwen, T., 2005. "Characterization of Fuel Composition Effects in H₂/CO/CH₄ Mixtures Upon Lean Blowout". No. GT2005-68907, ASME/IGTI Turbo Expo 2005.
- [11] Noble, D., Zhang, Q., Shareef, A., Tootle, J., Meyers, A., and Lieuwen, T., 2006. "Syngas Mixture Composition Effects Upon Flashback and Blowout". No. GT2006-90470, ASME/IGTI Turbo Expo 2006.
- [12] Lee, M., Seo, S., Chung, J., Kim, S., Joo, Y., and Ahn, D., 2010. "Gas turbine combustion performance test of hydrogen and carbon monoxide synthetic gas". *Fuel*, **89**, pp. 1485–1491.
- [13] Daniele, S., Jansohn, P., and Boulouchos, K., 2009. "Flame Front Characteristic and Turbulent Flame Speed of Lean Premixed Syngas Combustion at Gas Turbine Relevant Conditions". No. GT2009-59477, Proceedings of ASME Turbo Expo 2009.
- [14] Boschek, E., Griebel, P., and Jansohn, P., 2007. "Fuel Variability Effects on Turbulent Lean Premixed Flames at High Pressures". No. GT2007-27496, ASME/IGTI Turbo Expo 2007.
- [15] Richards, G., Straub, D., Ferguson, D., and Robey, E. "Chapter 5 Gas Turbines". In *LNG Interchangeability/Gas Quality: Results of the National Energy Technology Laboratory's Research for the FERC on Natural Gas Quality and Interchangeability*.
- [16] Juste, G., 2006. "Hydrogen injection as additional fuel in gas turbine combustor. Evaluation of effects". *International Journal of Hydrogen Energy*, **31**, pp. 2112–2121.
- [17] Barbosa, S., de la Cruz Garcia, M., Ducruix, S., Labégorre,

- B., and Lacas, F., 2007. "Control of combustion instabilities by local injection of hydrogen". Vol. 31, p. 3207C3214.
- [18] Altay, H., Hudgins, D., Speth, R., Annaswamy, A., and A.F., G., 2010. "Mitigation of thermoacoustic instability utilizing steady air injection near the flame anchoring zone". *Combustion and Flame*, **157**, pp. 686–700.
- [19] Schefer, R., White, C., and Keller, J., 2008. "Chapter 8: Lean Hydrogen Combustion". In *Lean Combustion Technology and Control*, D. Dunn-Rankin, ed. Academic Press, London, pp. 213–254.
- [20] Bouvet, N., Gökalp, I., Lee, S., and Santoro, R., 2007. "Laminar Flame Speed Study of Syngas Mixture (H₂-CO) with Straight and Nozzle Burners". No. AIAA 2007-5659, 43rd AIAA/ASME/SAE/ASEE Joint Propulsion Conference & Exhibit.